

Multimodal optical measurement for study of lower limb tissue viability in patients with diabetes mellitus

V.V. Dremi^{a*}, E.A. Zherebtsov^b, V.V. Sidorov^c, A.I. Krupatkin^d, I.N. Makovik^a,
A.I. Zherebtsova^a, E.V. Zharkikh^a, E.V. Potapova^a, A.V. Dunaev^a, A. Doronin^e,
A.V. Bykov^f, I.E. Rafailov^g, K.S. Litvinova^h, S.G. Sokolovski^b, E.U. Rafailov^b

^aOrel State University named after I.S. Turgenev, Scientific-Educational Center “Biomedical Engineering”, Orel, Russia, 302026

^bAston University, Optoelectronics and Biomedical Photonics Group, Aston Institute of Photonic Technologies, Birmingham, UK, B4 7ET

^cSPE “LAZMA” Ltd., Moscow, Russia, 125252

^dPriorov Central Research Institute of Traumatology and Orthopaedics, Moscow, Russia, 115172

^eYale University, Computer Graphics Group, Department of Computer Science, New Haven, United States, 06511

^fUniversity of Oulu, Optoelectronics and Measurement Techniques Laboratory, Faculty of Information Technology and Electrical Engineering, Oulu, Finland, FI-9014

^gAston University, School of Engineering and Applied Sciences, Aston Institute of Photonic Technologies, Birmingham, UK, B4 7ET

^hAston University, Aston Medical School, Birmingham, UK, B4 7ET

Abstract. According to the International Diabetes Federation, the challenges of early stage diagnosis and treatment effectiveness monitoring in diabetes is currently one of the highest priorities in modern healthcare. In this experimental study, the potential of combined measurements of skin fluorescence and blood perfusion by the laser Doppler flowmetry method in diagnostics of low limb diabetes complications was evaluated. With the use of Monte Carlo probabilistic modelling, the diagnostic volume and depth of the diagnosis were evaluated. The experimental study involved 76 patients with type 2 diabetes mellitus. These patients were divided into two groups depending on the degree of complications. The control group consisted of 48 healthy volunteers. The local thermal stimulation was selected as a stimulus on the blood microcirculation system. Experimental studies have shown that diabetic patients have elevated values of normalised fluorescence amplitudes, as well as a lower perfusion response to local heating. In the group of people with diabetes with trophic ulcers, these parameters also significantly differ from the control and diabetes only groups. Thus, the intensity of skin fluorescence and level of tissue blood perfusion can act as markers for various degrees of complications from the beginning of diabetes to the formation of trophic ulcers.

Keywords: fluorescence spectroscopy, metabolism, advanced glycation end products, mitochondrial function, laser Doppler flowmetry, diabetes mellitus, diagnostic volume.

*First Author, E-mail: dremi_viktor@mail.ru

1 Introduction

According to the International Diabetes Federation (IDF), the challenges of early stage diagnosis and monitoring of the treatment effectiveness in diabetes is currently one of the highest priorities in modern healthcare. The medical, social and economic significance of diabetes is primarily determined by the high prevalence of this disease and the frequency of debilitating and quality of

life reducing effects suffered by affected individuals. The IDF report for 2015 indicated that there are 415 million diabetic patients worldwide, with this figure projected to grow to 642 million by 2040.¹

Over the last several years, multiple studies have indicated that a timely diagnosis and treatment, including an increased level of patient monitoring, reduce the manifestation of various complications, potentially even reversing them at early pre-clinical stages. Particular attention is given to foot complications such as *peripheral arterial disease (PAD)*, neuropathy, skin disorders including foot ulcers, which are liable for more hospitalisations than any other complication of diabetes.² Particularly of interest, however, are vascular disorders such as *PAD*, which lead to the most adverse implications for patients. Macro- and microcirculatory disturbances, which are often imperceptibly formed, significantly reduce the patient's life quality. This can eventually lead to an early death of the patient. Disorders of microcirculation can occur long before the clinical manifestation of diabetes and play a central role in the development of foot ulcers and their subsequent inability to heal.³⁻⁷

Available diagnostic approaches for investigation of *PAD* at the level of macro- and microcirculation offer both advantages and disadvantages inherent to each method. Currently, the commonly employed standards of diabetic foot disorder detection in hospitals or surgery are predominantly thorough medical history examination, visual inspection and duplex ultrasonography scanning of arteries. The latter methods are capable of determining the level of trophic disorders, specifically of the haemodynamics. However, for microcirculatory disturbances, ultrasound Doppler is not efficient enough.⁸ Other methods like radiocontrast angiography have significant limitation during regular patient control: invasiveness, contrast agent toxicity and prolonged exposure of the patient to radiation.^{9,10} In addition to the methods, medical device

manufacturers offer solutions that allow for a joint diagnosis of macrovascular (measurement of Ankle Brachial Index (ABI), Toe Brachial Index (TBI), Pulse Volume Recording (PVR) and Segmental Pressure (SP) with measurement under ultrasonic or laser Doppler flowmetry control)^{11,12} and microvascular (transcutaneous oximetry) disorders. Often, this allows the acquisition of qualitative information about peripheral arterial diseases and assessment of the wound healing potential. However, the interpretation of the described parameters of vascular disorders can be somewhat subjective. The measurement results are affected by arterial calcifications as well as the rigidity of the vascular wall.¹³⁻¹⁵ Also, it is known that these methods can underestimate the true prevalence of cardiovascular diseases and, in particular, do not detect an early phase of vascular complications.¹⁶ The method of transcutaneous oximetry (TcPO₂) allows to assess the oxygen partial pressure in the intercellular liquids.^{17,18} Due to physiological, methodological and technical obstacles, this approach was not widely used in polyclinic diagnostics. At the same time, the trustworthiness of data obtained by this method could be questioned because of low selectivity to infectious inflammation on the foot, peripheral oedema and other accompanying pathologies.^{19,20} Another conventionally employed approach is thermal imaging, which reveals thermal asymmetry zones on the limb surface. The result of the diagnostics, however, is usually meaningful only during late stages of the limb angiopathy, when the blood circulation is damaged on the level of great vessels.^{21,22}

Additionally, to date, a general drawback of the methods available in the physician's arsenal is the inability to monitor the *metabolic processes* occurring in biological tissue. Patients with diabetes often display severe disorders of microcirculation, accompanied by significant metabolic shifts. Consequently, oxygen transport, its delivery and tissue consumption are the most important

indicators of the functioning of life support systems, and their adequate evaluation is important for choosing the optimal methods and tactics for treating each individual patient.

Despite this, there is little information on the effect of changes in blood flow in the delivery of oxygen and tissue metabolism of the lower limbs in diabetes mellitus. The influence of the development of diabetes on foot metabolism has not been practically investigated at present⁴. The main purpose of this article was to show a possible approach in assessing not only vascular disorders occurring in diabetes mellitus, but also associated metabolic disorders.

It is known that variations in the *respiratory chain* enzyme activities are recognised as one of the consequences resulting from a breach in the cell function observable in diabetes mellitus.²³⁻²⁵ Currently, a lot of research is being done to study the metabolism of epithelial tissues, including skin, using fluorescence spectroscopy and imaging techniques²⁶⁻³⁰. Changes in the mitochondrial respiratory chain are recognised as one of the consequences resulting from a breach in the cell function observable in different pathologies. The most likely changes to occur are the accumulation of a coenzyme NADH (the reduced form) and FAD (oxidized form). Detection of such changes by fluorescence spectroscopy is one of the most promising directions for *in vivo* diagnosis.

A recent review^{31,32} and some other studies shows that changes in the fluorescence of the NADH respiratory chain were measured in single cells^{33,34}, in tissue slices³⁵ and organs³⁶⁻³⁹. Despite the fact that study of NADH and FAD fluorescence has been successfully held for the past 50 years, relatively little research is conducted at the organ level. Meanwhile, the results of experiments on a particular organ or area of the body can be more successfully extrapolated to clinical practice in comparison to the studies at the cellular and subcellular level.

Furthermore, it has been established in recent years that long-existing diabetes with hyperglycaemia results in an increase in protein glycation levels. This is accompanied by an increase in so-called *advanced glycation end products (AGEs)*, which influence the properties of collagen and other structural proteins of the capillary membrane and skin.^{40–43} Among a number of AGE (e.g. N ϵ -carboxymethyllysine (CML), N ϵ -carboxyethyllysine (CEL), pyrrolidine, pentosidine, responsible for the formation of adhesions between collagen fibres, has its own fluorescence.^{44–46}

Thus, development of new optical diagnostic methods in these latter days has potential to find promising application in the diagnosing of diabetes disorders. The advantage of these methods lie in their non-invasive properties, good spatial resolution, low cost procedures and high productivity. One of the promising directions of optical diagnostics development is the establishment of a scientific and instrumental framework to create rapid and real-time *in vivo* analysis methods for determining biological tissue viability.⁴⁷

For a comprehensive diagnosis of the state of microcirculatory-tissue systems, it is currently promising to apply several diagnostic technologies simultaneously in one diagnostic volume.^{31,48,49} To assess the state of blood flow and detect possible vascular disorders, different combinations of methods are applied. For instance, simultaneous measurements of the intensities of fluorescence and Rayleigh components in human eye lenses allow a good accuracy to separate patients with diabetes from a control group.⁵⁰ Furthermore, diffuse reflectance spectroscopy (DRS) can be used for correction of the data obtained during fluorescence studies.^{51,52} Another example of combined technologies is a lightguide tissue spectrophotometry (O2C). It is a combination of LDF and tissue spectrometry. This method allows for the measurement of both relative blood flow by the laser

Doppler technique and haemoglobin oxygenation and haemoglobin amount in tissue by spectrometric techniques.⁵³

In this study, we experimentally estimate the potential of co-registering cutaneous blood flow parameters and the intrinsic tissue fluorophore fluorescence to distinguish stages of the complications of lower extremities in patients with diabetes mellitus. From the point of view of the fluorescence analysis, it is logical to consider a complex parameter, which describes the *oxidative metabolic processes* (changing the contents of NADH and FAD) and the *carbohydrate metabolism* (AGEs accumulation) in tissue, related to patients with diabetes manifesting as complications of the lower limbs.

2 Material and Methods

2.1 Experimental equipment

In the experimental studies, the tissue blood perfusion and the tissue fluorescence were assessed by LDF and FS respectively.⁵⁴ Registered perfusion parameters and the amplitude of the coenzymes' fluorescence were simultaneously evaluated using a specially designed system in the same tissue volume (SPE "LAZMA" Ltd, Russia). The Doppler channel built on the basis of the single mode laser module used a wavelength of 1064 nm. A 365 nm and 450 nm radiation sources were used for fluorescence excitation. A multi-optical fibre probe was used for delivery of penetrating radiation and registration of back reflected secondary radiation from the tissue (Fig. 1A). The probing fibre of the LDF channel has a diameter of 6 microns, the receiving fibre has a diameter of 400 microns.⁵⁵ The source-detector spacing for the LDF channel is 1.5 mm. In the FS channel, diameters of all probing and receiving fibres are 400 microns. For safety reasons, as well as to keep photobleaching of the tissue at an acceptable level, probe radiation power of the 365 nm

excitation wavelength at the output of the fibre probe did not exceed 1.5 mW. To assess the safety of the probe, coupled with the LED, we used documentation of the International Commission On Non-Ionizing Radiation Protection (ICNIRP)⁵⁶. The calculation gives the effective skin irradiance of 1.4 W/m². Accordingly the cited guideline document, the limiting UV exposure duration per day for the level of effective irradiance is at least 10 s. During this protocol, the actual time of the UV-irradiation did not exceed 1 s. Therefore, from the point of view of the ICNIRP recommendations, the proposed protocol of using of the probe was deemed to be safe. The output power for the 450 nm excitation wavelength did not exceed 3.5 mW. The source-detector spacing for the FS channel was 1 mm. The numerical aperture of the fibres was 0.22.

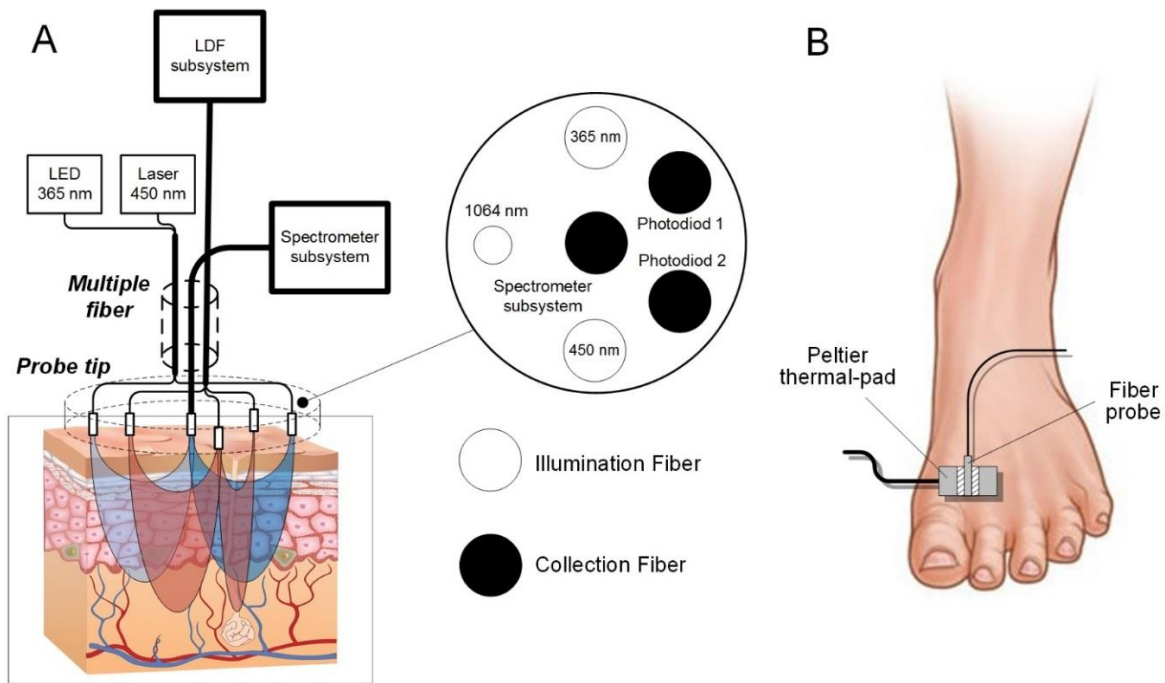


Fig. 1 The general scheme of the measuring system (A); localisation of the fibre optic probe with Peltier thermal-pad (B).

Specialised software was developed to work with the system. This allowed for real-time control of the course of the experiment and analysis of recorded parameters. It further allowed the control of the unit responsible for realising thermal functional tests.

2.2 Experimental Study

The experimental study involved 76 patients with Caucasian skin type and with type 2 diabetes mellitus at the Endocrinology Department of the “Orel Regional Clinical Hospital” (Orel, Russia). The study did not include volunteers with cardiovascular, bronchopulmonary or neuroendocrine system disease comorbidities, nor with diseases of the gastrointestinal tract, liver, kidneys, blood and any other serious chronic diseases, which could have an impact on the diagnostic results. Volunteers with a history of alcoholism, drug addiction and drug abuse were also excluded. Laboratory parameters were measured according to standard laboratory procedures. The measurement of blood pressure was carried out after 5 minutes of rest, with the patient in a sitting position. 14 people from the patient's group were considered to have a more severe course of the disease (Diabetic group 2). The decision on the degree of severity in each case was taken based on the presence of trophic disorders in the form of ulcers, analysis of anamnesis and consultation with the attending physician. Thus, Diabetic group 2 consisted of all diabetics with the presence of visible trophic ulcers, Diabetic group 1 included patients without trophic ulcers. Patients were examined on the first day of admission to the clinic. Prior to hospitalisation, patients took medication to reduce high blood glucose levels. The control group consisted of 48 healthy volunteers (mean age 46 ± 6 years). The participating volunteer group was collected through an internal university advertisement circulated by physical posters and notification email. The experiments were conducted under established protocols. The study protocol was approved at a meeting of the ethics committee at Orel State University named after I.S. Turgenev from 03/11/2015 (minutes of the meeting №7). After receiving the description of the protocol, all participating volunteers signed an informed consent form.

The main characteristics of the studied groups are presented in Table 1. With a specified probability of 0.01, we can consider that the compared groups are statistically homogeneous with a difference in fasting glucose level and body mass index. The table shows that the Diabetic group 2 had a longer duration of diabetes, higher values of creatinine and urea (which may indicate kidney function is decreased), but these parameters did not reach statistically significant level ($p > 0.01$). However, the percentage of complications in this group (diabetic polyneuropathy, diabetic retinopathy, diabetic nephropathy, diabetic microangiopathy of the lower limbs) is statistically significant compared to the Diabetic group 1.

Table 1 Statistical difference between patient groups and data for controls.

Characteristics	Diabetic group 1	Diabetic group 2	Control group	P Value
Sex, M/F	20/42	8/6	30/18	0.08
Age, y	54±10	53±13	46±6	0.89
Systolic BP, mmHg	136±16	144±22	128±9	0.29
Diastolic BP, mmHg	83±8	85±8	80±5	0.12
Body mass index, kg/m ²	31.9±6.3	32.0±6.2	24.2±2.5	<0.001*
Fasting glucose (mmol/l)	9.3±4.8	9.1±2.5	4.8±0.4	<0.001*
Diabetes duration, y	11±7	18±12	–	0.03**
HbA1c, %	8.6±1.5	8.6±0.7	–	0.28**
HbA1c, mmol/mol	70±9	70±4	–	0.31**
Total cholesterol, mmol/l	4.9±1.2	5.1±1.3	–	0.76**
Creatinine, umol/l	81.5±28.7	90.3±16.9	–	0.02**
Urea, mmol/l	7.7±6.8	8.2±2.3	–	0.09**
ALT, IU/L	34.2±20.3	28.4±19.3	–	0.25**
AST, IU/L	31.0±24.8	24.1±13.4	–	0.13**
The presence of complications, % of the total number of patients	15	50	–	0.007**

Data are mean±SD unless stated otherwise. *Control group vs Diabetic group 1 and Diabetic group 2. ** Diabetic group 1 vs Diabetic group 2. Nonparametric data of the three studied groups were analysed by a Kruskal-Wallis ANOVA. A Mann-Whitney U-test test was used to identify differences between the two groups. Reference values of the laboratory: HbA1c 4.0-6.0 %, total cholesterol 3.5-5.0 mmol/l, urea 2.5-7.5 mmol/l, creatinine 70-110 µmol/l, ALT 10-38 IU/L, AST 10-40 IU/L.

The local heating stimulation was selected as a provocative action on the blood microcirculation system, allowing assessment of the local regulatory mechanisms of blood flow. Using a special block “LAZMA-TEST” (SPE “LAZMA” Ltd., Russia), a consecutive local cold (25 °C) and heat (35 °C and 42 °C) provocations were applied for 4 minutes each. The first stage included registration of microcirculatory parameters in the basal conditions for a 4 minute period and the recording of a pair of fluorescence spectra. Thus, the duration of one study was approximately 16 minutes.

In the study, the probe was secured on the dorsal surface of the foot to a point located on a plateau between the 1st and 2nd metatarsal bones (Fig. 1B). We investigated the area of nonglabrous skin, where changes in blood flow are mediated by the vessels themselves and by two mechanisms of the sympathetic nervous system: noradrenergic vasoconstrictor nerves and a cholinergic active vasodilator system.⁵⁷ It is due to this that the bulk of the literature^{58,59} is focused on controls of the nonglabrous skin with less focus on the glabrous skin of the palms, soles, and digits. Moreover, some research stated that perfusion in the sites with arteriovenous anastomoses (with glabrous or non-hairy skin) may fluctuate substantially^{60,61}, so the microcirculation assessment in this area may not be a very sensitive indicator of disease severity.⁶² Particular attention was paid to minimise a local pressure of the probe on skin, as the parameter strongly influences on the measurement results of skin blood perfusion and fluorescence intensity.⁶³ All studies were performed in the supine position. The volunteers were asked to refrain from food and drink 2 hours before the study to exclude the influence of these factors on the change of microhemocirculation and metabolic processes. Room temperature was maintained at a steady 24-25 °C. All volunteers underwent preliminary adaptation to these conditions for at least 10 min. Furthermore, skin temperature change of volunteers was recorded during the study. In the basal

conditions, subjects had different skin temperatures. In this regard, to unify measurements, we pre-cooled the study area on the foot to 25 °C.

2.3 Validation of diagnostic depth of the probe

Proper evaluation of fluorescence intensity measurements in healthy tissue and areas of pathology will be possible if the penetration depth of the radiation, as well as diagnostic volume, were known. It is also important for the researcher or practising physician to understand the depth of penetration of probing radiation in laser Doppler measurements for a specific measuring device.⁶⁴ This would provide information on the blood vessels involved in the formation of the signal.

Due to the complexity of the actual sensing conditions, as well as a complex composite structure of human skin, it is not possible to obtain a general analytical solution to evaluate the diagnostic volume. In this regard, the method of stochastic Monte Carlo (MC) simulations was used. Currently, there are some known realisations of this approach used to simulate the propagation of optical radiation in organic tissues.⁶⁵⁻⁶⁷ One of the more advanced approaches is the use of an object-oriented MC model,⁶⁸⁻⁷¹ which allows for the description of the photons and the structural components of the tissue as independent objects interacting with each other. For acceleration of simulation performance, parallel computing was implemented on the used algorithms. Parallel computing technology CUDA (Computer Unified Device Architecture, NVIDIA Corporation) was employed as a framework of the calculations.

For both the LDF measurements and the fluorescence measurements the diagnostic volume was assessed through an evaluation of the probe radiation distribution. For fluorescence measurements, the validity of this approach is based on the fact that, according to the rule of Stokes shift, the fluorescence spectrum is shifted into the long-wave region. It is also known, that the absorption of light in most of the biological tissues for wavelengths of visible spectrum falls as

wavelength increases. Thus, to get a lower-bound estimate of the diagnostic volume of the measurements, it is sufficient to assess the sampling volume of the radiation for a wavelength of fluorescence excitation. One of the possible ways to formalise calculation of the sampling volume is calculating the distribution of rays reaching the detector using the Monte Carlo method.

A seven layer tissue model was used to simulate the diagnostic volume and depth of penetration of the probe radiation. This model was originally proposed in the paper.⁶⁸ Fig. 2A shows an example of the distribution obtained for the above simulation parameters for a wavelength of 365 nm. Thus, diagnostic depth of the conducted diagnostics is at least several hundred microns and includes the epidermis, papillary dermis layer and small part of upper blood net dermis (Fig. 2A). Diagnostic volume, estimated by simulation, is in the order of 0.2 mm³.

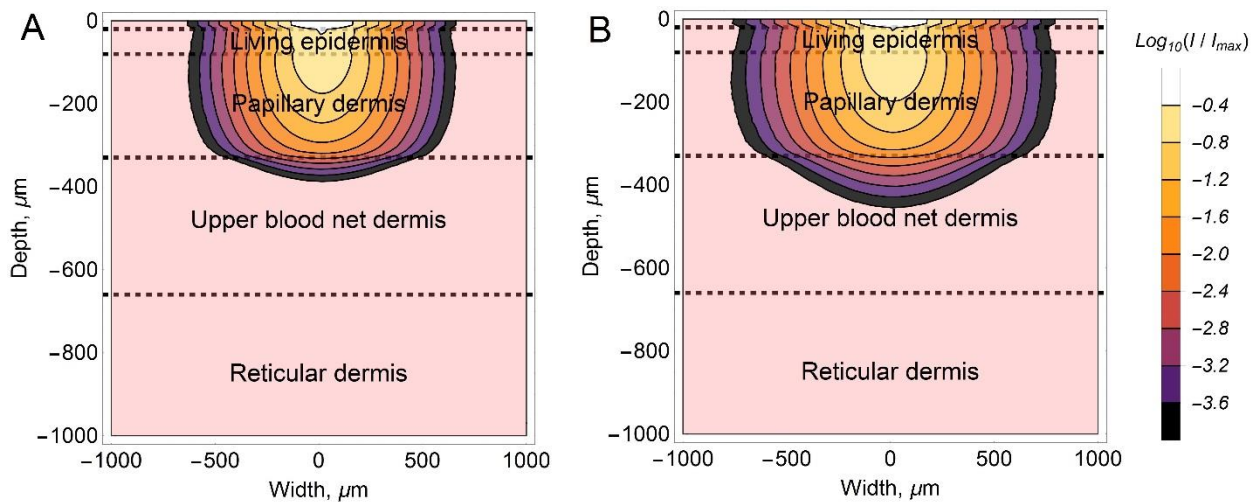


Fig. 2 Result of the modelling of diagnostic volume for the fluorescence measurements for the excitation wavelength of 365 nm (A) and 450 nm (B) for the parameters of the used optical fibre probe: the distance between the fibres – 1 mm, fibre diameter – 400 microns, receiving aperture angle – 0.22.

For an excitation wavelength of 450 nm, diagnostic depth reaches 450-500 microns and penetrates the epidermis, papillary dermis and most of the upper blood net dermis (Fig. 2B). In this case, the diagnostic volume is approximately estimated by the simulation as 0.35 mm³.

The performed simulation shows that the proposed probe allows for the registration of fluorescence in the epidermis, mainly contributed to by NADH and FAD, and the dermis with a significant contribution from collagen.

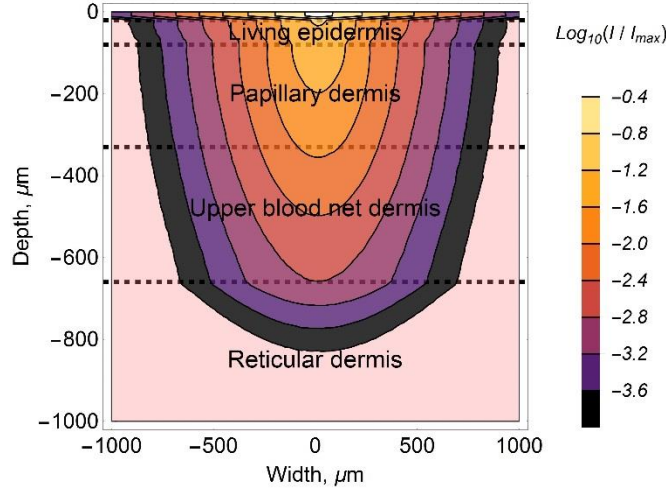


Fig. 3 The result of modelling the diagnostic volume for the LDF measurements for the wavelength of 1064 nm, using the following optical fibre probe parameters: distance between the fibres – 1.5 mm, receiving aperture angle – 0.22.

The results of diagnostic volume modelling for the LDF probe show that the value is about 1.8 mm³. This confirms that this probe of the developed device is highly sensitive to the variations of blood flows in the papillary dermis, upper blood net plexus and able to cover the top part of the reticular dermis (Fig. 3).

2.4 Data Analysis

The recorded and subsequently averaged amplitudes AF_{460} of the fluorescence at 460 ± 10 nm with excitation at 365 nm and AF_{525} of the fluorescence at 525 ± 10 nm with excitation at 450 nm (normalized to the intensity of the backscattered excitation radiation), as well as the average blood tissue perfusion I_m at each stage of the functional test, were analysed. The wavelengths were selected to maximise the probability of detection of NADH and FAD signals. Taking into account the relatively small sample sizes, nonparametric methods were used to confirm the reliability of

differences in the results even in small groups of observations, namely the Mann-Whitney U-test and Kruskal-Walles ANOVA test. Values of $p < 0.01$ were considered significant.

Considering the former division of experimental data into classes (two patient and one control), a linear discriminant analysis was employed to determine the discriminant function, leading to the synthesis of the desired decision rule. The obtained classifiers allow for a reappearing object to be assigned to one of the above classes by measured parameter values. Evaluation of the discriminant analysis quality was performed using the ROC-curve.

3 Experimental Results and Discussion

3.1 Experimental Study

Experimental studies have shown that diabetic patients have elevated values of normalised fluorescence amplitudes, as well as a lower perfusion response to local heating (up to 35 and 42 °C). At the same time, in the group of diabetic patients with trophic ulcers (Diabetic group 2), these parameters also significantly differ from the control and diabetes only groups (Table 2, Fig. 4).

Table 2 The results of experimental studies.

Parameter	Control group	Diabetic group 1	Diabetic group 2
Fluorescence amplitude AF_{460} , AU	2.1±0.8	2.7±0.8*	3.8±0.7**
Fluorescence amplitude AF_{525} , AU	1.2±0.4	1.8±0.7*	2.5±0.6**
Perfusion I_m , PU	5.0±1.9	5.3±2.2	3.8±1.6
Perfusion $I_m^{25\text{ }^\circ\text{C}}$, PU	4.4±1.6	4.7±2.0	3.6±1.4
Perfusion $I_m^{35\text{ }^\circ\text{C}}$, PU	8.7±3.1	6.6±2.4*	5.0±1.4**
Perfusion $I_m^{42\text{ }^\circ\text{C}}$, PU	19.9±4.6	12.3±3.5*	9.2±4.6**

* – Confirmed statistically significant differences between Control group and Diabetic group 1 ($p < 0.01$)

** – Confirmed statistically significant differences between Diabetic group 1 and Diabetic group 2 ($p < 0.01$)

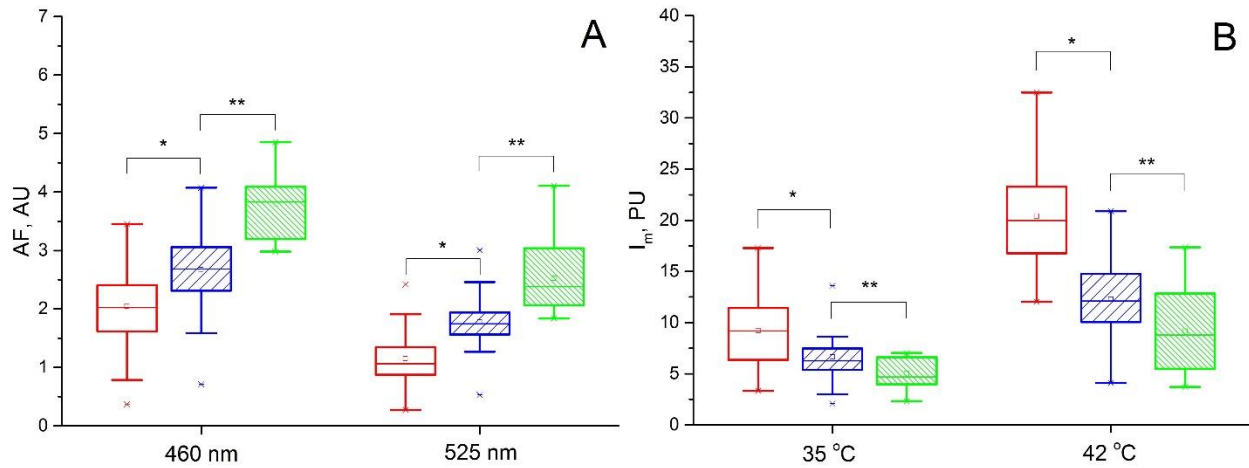


Fig. 4 Comparison of parameters between control (red empty bars), diabetic (blue loose shading) and diabetic with ulcers (green tight shading) groups: the normalised fluorescence amplitude (A) and the average perfusion in the stages of heating to 35 and 42 °C (B). In each box, the central line is the median of the group, while the edges are the 25th and 75th percentiles.

As already mentioned, AGEs contribute to the mechanisms responsible for the development of complications in diabetes. Formation of intracellular AGEs promotes violation in protein function, with their accumulation acting as an objective marker for the tissues glycation. The level of skin fluorescence observed in our studies is related to the degree of conventional glycation marker HbA1c as determined *in vitro*. It is important to note, however, that the standard measure of glycation using HbA1c, characterises the glycation processes that occur only in the short term (around three months). Changes in AGE content reflect long-term processes in the diabetic skin. Considering the long molecular lifetime of collagen and the stability of AGEs, it is possible to use skin fluorescence as a measure of the total impact of hyperglycaemia throughout the course of life.

It is known that diabetes can lead to tissue hypoxia.⁷²⁻⁷⁴ In the event of hypoxia, the aerobic cellular respiration pathway is disrupted, and the mitochondrial NADH oxidation is slowed down. Additionally, the glycolysis pathway for NADH formation is activated. In this context, the accumulation of NADH may act as a sign of tissue hypoxia, with its contribution to the total fluorescence signal serving as a marker of total oxygen deficiency in tissues. Meanwhile, the

processes of oxidative phosphorylation exhibit changes in the concentrations of NADH and FAD, which are very complex and the dynamics of these changes may be nonlinear throughout the cell's lifetime.^{38,39} This should be taken into account when interpreting the data received and further research in this area.

It is also shown that the accumulation of AGEs may suppress the synthesis of NO in endothelial cells.⁷⁵⁻⁷⁷ This may also explain the differences in perfusion response to various stimuli. Basal level does not statistically differ between the compared groups. However, the proposed functional stimulation in the form of thermal tests can detect and distinguish between microvascular abnormalities in diabetic patients. The perfusion increase during a local heating test occurs mainly due to two mechanisms. The heating of skin to 34-35 °C results in activation of peptidergic nerve fibres. This happens due to the activation of thermosensitive TRPV1 receptors.⁷⁸ The vasodilation caused by heating skin to 42 °C is associated with a release of NO from vascular endothelium.^{79,80} Topographically, both arterioles and capillaries are involved in local heating. All aspects of the microvasculature and tissue systems undergo dysfunction during diabetes, including the vascular endothelial and perivascular nerve fibres. Therefore, the thermal test is pathogenically justified for diagnosing these disorders during diabetes. A reduction in perfusion growth when skin is heated to 35 °C acts as an objective criterion of sensory nerve fibre dysfunction, which in turn serves as a component of diabetic neuropathy. The reduction of perfusion growth in people with diabetes compared with the control group during skin heating to 42 °C reflects a deficit of endothelium-dependent vasodilation mechanisms (presumably NO-induced).

3.2 *Data Analysis*

The analysed parameters of normalised skin fluorescence amplitudes and perfusion are proposed for the synthesis of the decision rule. As stated above, these parameters satisfy the principles of

statistical independence, as well as the significance of the differences of their values, calculated for the patients' and control groups. The discriminant function is synthesised in such a way as to provide high sensitivity while providing excellent specificity. Table 3 summarises the sensitivity and specificity for the first classification rule (the control group is compared with a group of patients without ulcers) for a different combination of measured parameters. As can be seen from the table, the lowest level of error is obtained with the combination of fluorescence intensity at an excitation wavelength of 365 nm and the level of stimulation of microcirculatory perfusion at 42 °C.

Table 3 Sensitivity and specificity for the first classification rule.

Parameter	AF_{460}	AF_{525}	$I_m^{35\text{ }^\circ\text{C}}$	$I_m^{42\text{ }^\circ\text{C}}$	$AF_{460},$ $I_m^{35\text{ }^\circ\text{C}}$	$AF_{460},$ $I_m^{42\text{ }^\circ\text{C}}$	$AF_{525},$ $I_m^{35\text{ }^\circ\text{C}}$	$AF_{525},$ $I_m^{42\text{ }^\circ\text{C}}$
Sensitivity	0.64	0.77	0.77	0.88	0.75	0.92	0.87	0.90
Specificity	0.7	0.79	0.62	0.81	0.77	0.90	0.77	0.83

For the second classification rule for the separation of the diabetic group and diabetic group with ulcers, a sensitivity and specificity of 0.86 and 0.85, respectively, were obtained. For better combinations of sensitivity and specificity, Fig. 5A shows the scatter plot of experimental data with applied discriminant lines that divide the experimental points into three groups (healthy, diabetic and diabetic with ulcers). The immediate diagnostic criterion, with the aid of the discriminant functions (D_1 and D_2), allows for the relation of a newly measured subject to one of the three groups:

$$\begin{cases} D1 = -2.55 - 0.45AF_{460} + 0.23I_m^{42^\circ\text{C}}, \\ D2 = -1.8 + 1.16AF_{460} - 0.18I_m^{42^\circ\text{C}}. \end{cases} \quad (1)$$

It can be seen from Fig. 5A that the shift towards the top-left characterises the deterioration of the patient's condition and increasing the risk of development of foot ulcers.

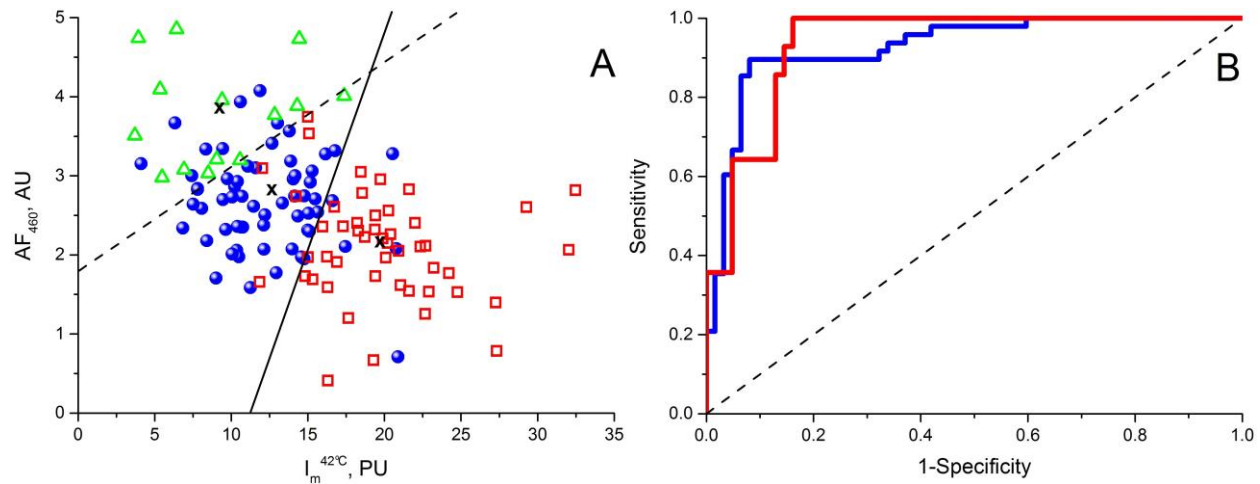


Fig. 5 The scatter plot with applied discriminant lines, obtained by linear discriminant analysis method (A) and ROC-curves for assessing the effectiveness of the classifiers (B). The healthy group is shown by squares, diabetic group – circles, the diabetic group with ulcers – triangles. For the ROC curve: red line – Control group vs Diabetic group 1, the blue line – Diabetic group 1 vs Diabetic group 2.

Fig. 5B shows the ROC-curves calculated for the obtained discriminant functions. To compare the quality of different classifying rules, it is convenient to use the integral characteristic AUC – Area under Curve. In our case, for both classification rules – AUC=0.93. This indicator indicates a high level of quality of the classifier.

Thus, the skin fluorescence and level of tissue blood perfusion during a local heating test can act as markers for various stages of diabetes, beginning with early disease, to the advancement and development of trophic ulcers.

4 Conclusion

The obtained experimental results confirm the prospects of the development of new methods for evaluating metabolic shifts in diabetes mellitus. The proposed method could be a marker of diabetic complications. It can also be used to assess therapeutic interventions aimed at preventing or reversing the progression of these diabetic complications.

Modelling and experimental results of this study confirm the high sensitivity of optical non-invasive methods (laser Doppler flowmetry and fluorescence spectroscopy) when detecting violations of biological tissue in type 2 diabetes mellitus. Both approaches, either individually or in combination, may have important clinical implications as they may help to identify patients at risk of developing future problems within their lower limbs.

Improvement of methodological support of optical non-invasive diagnosis (convenient and completely safe for the patient) will make a significant contribution to the fight against diabetes, which is very relevant given the prevalence of the disease.

There is also further potential to expand the number of clinical investigations and improve the methodology. This will eventually allow the methods in question to be introduced into the practice of the attending physician.

A promising direction for future research within this field is the differentiation of AGEs and NADH and FAD contributions to the resultant fluorescence signal. This would allow for separate studies into the possible pathways of biological tissue violation: by oxidative phosphorylation and carbohydrate metabolism.

Acknowledgments

The work was supported by grant of the President of the Russian Federation for state support of young Russian scientists № MK-7168.2016.8. Authors acknowledge the support of the Academy of Finland (grants: 296408 and 290596). EAZ also acknowledged for personal support H2020 MCSA-funded project No. 703145. The authors would like to acknowledge the patients and volunteers. Special thanks are extended to doctors Alimicheva E.A., Masalygina G.I. and Muradyan V.F. of the “Orel Regional Clinical Hospital” for providing useful advice and help.

Duality of Interest

No potential conflicts of interest relevant to this article were reported.

References

1. *IDF Diabetes Atlas - 7th edition*, International Diabetes Federation (2015).
2. J. B. Rice et al., “Burden of diabetic foot ulcers for medicare and private insurers,” *Diabetes Care* **37**(3), 651–658 (2014).
3. S. Zimny et al., “Early Detection of Microcirculatory Impairment in Diabetic Patients With Foot at Risk,” *Journal Article, Diabetes Care* **24**(10), 1810 (2001).
4. R. L. Greenman et al., “Early changes in the skin microcirculation and muscle metabolism of the diabetic foot,” *Lancet* **366**(9498), 1711–1717 (2005).
5. J. Cobb and D. Claremont, “Noninvasive Measurement Techniques for Monitoring of Microvascular Function in the Diabetic Foot,” *Int. J. Low. Extrem. Wounds* **1**(3), 161–169 (2002).
6. P. Zhang et al., “Global epidemiology of diabetic foot ulceration: a systematic review and meta-analysis dagger,” *Ann. Med.* **49**(2), 106–116 (2017).
7. J. Z. M. Lim, N. S. L. Ng, and C. Thomas, “Prevention and treatment of diabetic foot ulcers,” *J. R. Soc. Med.* **110**(3), 104–109 (2017).
8. M. E. Ahmadi et al., “Neuropathic arthropathy of the foot with and without superimposed osteomyelitis: MR imaging characteristics,” *Radiology* **238**(2), 622–631 (2006).
9. D. S. Chatha, P. M. Cunningham, and M. E. Schweitzer, “MR imaging of the diabetic foot: diagnostic challenges,” *Radiol Clin North Am* **43**(4), 747–59, ix (2005).
10. N. Prandini et al., “Nuclear medicine imaging of bone infections,” *Nucl Med Commun* **27**(8), 633–644 (2006).

11. D. T. Ubbink, "Toe blood pressure measurements in patients suspected of leg ischaemia: a new laser Doppler device compared with photoplethysmography.," *Journal Article, Eur. J. Vasc. Endovasc. Surg.* **27**(6), 629–634 (2004).
12. J. C. de Graaff et al., "The usefulness of a laser Doppler in the measurement of toe blood pressures," *J. Vasc. Surg.* **32**(6), 1172–1179 (2000).
13. L. Ryden et al., "ESC Guidelines on diabetes, pre-diabetes, and cardiovascular diseases developed in collaboration with the EASD: the Task Force on diabetes, pre-diabetes, and cardiovascular diseases of the European Society of Cardiology (ESC) and developed in collaboratio," *Eur. Heart J.* **34**(39), 3035–3087 (2013).
14. N. M. J. Hanssen et al., "Associations between the ankle-brachial index and cardiovascular and all-cause mortality are similar in individuals without and with type 2 diabetes: nineteen-year follow-up of a population-based cohort study.," *Diabetes Care* **35**(8), 1731–1735 (2012).
15. J. Haraden and C. Jaenicke, "Correlation of preoperative ankle-brachial index and pulse volume recording with impaired saphenous vein incisional wound healing post coronary artery bypass surgery.," *J. Vasc. Nurs.* **24**(2), 35–45 (2006).
16. C. Hoyer, J. Sandermann, and L. J. Petersen, "The toe-brachial index in the diagnosis of peripheral arterial disease.," *J. Vasc. Surg.* **58**(1), 231–238 (2013).
17. K. Huang et al., "The correlation between transcutaneous oxygen tension and microvascular complications in type 2 diabetic patients," *J. Diabetes Complications* **31**(5), 886–890 (2017).
18. P. Poredoš, "Validity of transcutaneous oxygen measurement in peripheral arterial disease," *Int. Angiol.* **36**(4), 392–393 (2017).

19. C. E. Fife et al., “Transcutaneous oximetry in clinical practice: consensus statements from an expert panel based on evidence,” *Undersea Hyperb Med* **36**(1), 43–53 (2009).
20. K. A. Arsenault et al., “The use of transcutaneous oximetry to predict healing complications of lower limb amputations: a systematic review and meta-analysis,” *Eur J Vasc Endovasc Surg* **43**(3), 329–336 (2012).
21. A. R. Berendt and B. Lipsky, “Is this bone infected or not? Differentiating neuro-osteoarthropathy from osteomyelitis in the diabetic foot,” *Curr Diab Rep* **4**(6), 424–429 (2004).
22. A. J. Boulton and L. Vileikyte, “The diabetic foot: the scope of the problem,” *J Fam Pr.* **49**(11 Suppl), S3-8 (2000).
23. S.-J. Lin and L. Guarente, “Nicotinamide adenine dinucleotide, a metabolic regulator of transcription, longevity and disease.,” *Curr. Opin. Cell Biol.* **15**(2), 241–246 (2003).
24. J. H. Hwang et al., “Pharmacological stimulation of NADH oxidation ameliorates obesity and related phenotypes in mice.,” *Diabetes* **58**(4), 965–974, (2009).
25. Y. Ido, C. Kilo, and J. R. Williamson, “Cytosolic NADH/NAD⁺, free radicals, and vascular dysfunction in early diabetes mellitus.,” *Diabetologia* **40 Suppl 2**, S115-7 (1997).
26. A. A. Heikal, “Intracellular coenzymes as natural biomarkers for metabolic activities and mitochondrial anomalies.,” *Biomark. Med.* **4**(2), 241–263 (2010).
27. D. Pouli et al., “Imaging mitochondrial dynamics in human skin reveals depth-dependent hypoxia and malignant potential for diagnosis.,” *Sci. Transl. Med.* **8**(367), 367ra169 (2016).
28. N. Rajaram et al., “Pilot clinical study for quantitative spectral diagnosis of non-melanoma skin cancer.,” *Lasers Surg. Med.* **42**(10), 716–727 (2010).

29. M. Balu et al., "In vivo multiphoton NADH fluorescence reveals depth-dependent keratinocyte metabolism in human skin.," *Biophys. J.* **104**(1), 258–267 (2013).
30. C. Li et al., "Multiphoton Microscopy of Live Tissues With Ultraviolet Autofluorescence," in *IEEE Journal of Selected Topics in Quantum Electronics* **16**(3), 516–523 (2010).
31. A. Mayevsky and B. Chance, "Oxidation-reduction states of NADH in vivo: from animals to clinical use," *Mitochondrion* **7**(5), 330–339 (2007).
32. A. Mayevsky and G. G. Rogatsky, "Mitochondrial function in vivo evaluated by NADH fluorescence: from animal models to human studies.," *Am. J. Physiol. Cell Physiol.* **292**(2), C615-40 (2007).
33. E. T. Obi-Tabot et al., "Changes in hepatocyte NADH fluorescence during prolonged hypoxia.," *J. Surg. Res.* **55**(6), 575–580 (1993).
34. F. Bartolome and A. Y. Abramov, "Measurement of mitochondrial NADH and FAD autofluorescence in live cells," *Methods Mol Biol* **1264**, 263–270 (2015).
35. K. A. Foster, C. J. Beaver, and D. A. Turner, "Interaction between tissue oxygen tension and NADH imaging during synaptic stimulation and hypoxia in rat hippocampal slices.," *Neuroscience* **132**(3), 645–657 (2005).
36. I. J. Rampil, L. Litt, and A. Mayevsky, "Correlated, simultaneous, multiple-wavelength optical monitoring in vivo of localized cerebrocortical NADH and brain microvessel hemoglobin oxygen saturation.," *J. Clin. Monit.* **8**(3), 216–225 (1992).
37. G. Papayan, N. Petrishchev, and M. Galagudza, "Autofluorescence spectroscopy for NADH and flavoproteins redox state monitoring in the isolated rat heart subjected to ischemia-reperfusion," *Photodiagnosis Photodyn Ther* **11**(3), 400–408 (2014).

38. M. Aldakkak et al., “Modulation of mitochondrial bioenergetics in the isolated Guinea pig beating heart by potassium and lidocaine cardioplegia: implications for cardioprotection,” *J Cardiovasc Pharmacol* **54**(4), 298–309 (2009).
39. J. An et al., “Warm ischemic preconditioning improves mitochondrial redox balance during and after mild hypothermic ischemia in guinea pig isolated hearts,” *Am J Physiol Hear. Circ Physiol* **288**(6), H2620-7 (2005).
40. P. Gkogkolou and M. Bohm, “Advanced glycation end products: Key players in skin aging?,” *Dermatoendocrinol* **4**(3), 259–270 (2012).
41. R. Meerwaldt et al., “Simple non-invasive assessment of advanced glycation endproduct accumulation,” *Diabetologia* **47**(7), 1324–1330 (2004).
42. K. C. Tan et al., “Advanced glycation end products and endothelial dysfunction in type 2 diabetes,” *Diabetes Care* **25**(6), 1055–1059 (2002).
43. E. G. Gerrits et al., “Skin autofluorescence: a tool to identify type 2 diabetic patients at risk for developing microvascular complications,” *Diabetes Care* **31**(3), 517–521 (2008).
44. D. R. Sell et al., “Pentosidine: a molecular marker for the cumulative damage to proteins in diabetes, aging, and uremia,” *Diabetes Metab Rev* **7**(4), 239–251 (1991).
45. D. R. Sell et al., “Pentosidine formation in skin correlates with severity of complications in individuals with long-standing IDDM,” *Diabetes* **41**(10), 1286–1292, (1992).
46. M. Takahashi et al., “Direct measurement of crosslinks, pyridinoline, deoxypyridinoline, and pentosidine, in the hydrolysate of tissues using high-performance liquid chromatography,” *Anal. Biochem.* **232**(2), 158–162, (1995).
47. V. V Tuchin, *Handbook of Photonics for Biomedical Science*, CRC Press (2010).
48. E. A. Zherebtsov et al., “Combined use of laser Doppler flowmetry and skin thermometry

- for functional diagnostics of intradermal finger vessels,” *J. Biomed. Opt.* **22**(4), 40502 (2017).
49. A. I. Zhrebtsova et al., “Study of the functional state of peripheral vessels in fingers of rheumatological patients by means of laser Doppler flowmetry and cutaneous thermometry measurements,” *Proc. SPIE* **9917**, 99170M (2016).
 50. N.-T. Yu et al., “Development of a noninvasive diabetes screening device using the ratio of fluorescence to Rayleigh scattered light,” *J. Biomed. Opt.* **1**(3), 280–288 (1996).
 51. V. V Dremmin et al., “The development of attenuation compensation models of fluorescence spectroscopy signals,” *Proc. SPIE* **9917**, 99170Y (2016).
 52. A. V Dunaev et al., “Individual variability analysis of fluorescence parameters measured in skin with different levels of nutritive blood flow,” *Med Eng Phys* **37**(6), 574–583 (2015).
 53. S. Beckert et al., “The Impact of the Micro-Lightguide O2C for the Quantification of Tissue Ischemia in Diabetic Foot Ulcers,” *Diabetes Care* **27**(12), 2863 (2004).
 54. V. V Dremmin et al., “The blood perfusion and NADH/FAD content combined analysis in patients with diabetes foot,” *Proc. SPIE* **9698**, 969810 (2016).
 55. A. V. Dunaev et al., “Novel measure for the calibration of laser Doppler flowmetry devices,” *Proc. SPIE* **8936**, 89360D (2014).
 56. “Guidelines on limits of exposure to ultraviolet radiation of wavelengths between 180 nm and 400 nm (incoherent optical radiation),” *Health Phys.* **87**(2), 171–186 (2004).
 57. J. M. Johnson and D. W. Proppe, “Cardiovascular Adjustments to Heat Stress,” in *Comprehensive Physiology* (2010).
 58. I. Fredriksson et al., “Reduced Arteriovenous Shunting Capacity After Local Heating and

- Redistribution of Baseline Skin Blood Flow in Type 2 Diabetes Assessed With Velocity-Resolved Quantitative Laser Doppler Flowmetry,” *Diabetes* **59**(7), 1578–1584 (2010).
59. Y.-K. Jan et al., “Skin blood flow response to locally applied mechanical and thermal stresses in the diabetic foot,” *Microvasc. Res.* **89**, 40–46 (2013).
 60. M. Thoresen and L. Walloe, “Skin blood flow in humans as a function of environmental temperature measured by ultrasound,” *Acta Physiol. Scand.* **109**(3), 333–341 (1980).
 61. L. Vanggaard et al., “Thermal responses to whole-body cooling in air with special reference to arteriovenous anastomoses in fingers,” *Clin. Physiol. Funct. Imaging* **32**(6), 463–469, (2012).
 62. D. Fuchs et al., “The association between diabetes and dermal microvascular dysfunction non-invasively assessed by laser Doppler with local thermal hyperemia: a systematic review with meta-analysis,” *Cardiovasc. Diabetol.* **16**(11) (2017).
 63. E. A. Zharebtsov et al., “The influence of local pressure on evaluation parameters of skin blood perfusion and fluorescence,” *Proc. SPIE* **10336**, 1033608 (2017).
 64. A. V Dunaev et al., “Substantiation of medical and technical requirements for noninvasive spectrophotometric diagnostic devices,” *J Biomed Opt* **18**(10), 107009 (2013).
 65. I. E. Rafailov et al., “Computational model of bladder tissue based on its measured optical properties,” *J. Biomed. Opt.* **21**(2), 25006 (2016).
 66. V. V Dremin and A. V Dunaev, “How the melanin concentration in the skin affects the fluorescence-spectroscopy signal formation,” *J. Opt. Technol.* **83**(1), 43–48 (2016).
 67. C. Zhu and Q. Liu, “Review of Monte Carlo modeling of light transport in tissues,” *J. Biomed. Opt.* **18**(5), 50902 (2013).
 68. G. I. Petrov et al., “Human tissue color as viewed in high dynamic range optical spectral

- transmission measurements,” *Biomed. Opt. Express* **3**(9), 2154–2161 (2012).
69. I. V Meglinski and S. D. Matcher, “Analysis of the spatial distribution of detector sensitivity in a multilayer randomly inhomogeneous medium with strong light scattering and absorption by the Monte Carlo method,” *Opt. Spectrosc.* **91**(4), 654–659 (2001).
 70. I. V Meglinsky and S. J. Matcher, “Modelling the sampling volume for skin blood oxygenation measurements,” *Med. Biol. Eng. Comput.* **39**(1), 44–50 (2001).
 71. I. Meglinski and A. Doronin, “Monte Carlo Modeling of Photon Migration for the Needs of Biomedical Optics and Biophotonics,” Chap. 1 in *Advanced Biophotonics*, pp. 1–72, Taylor & Francis (2013).
 72. L. Xi, C.-M. Chow, and X. Kong, “Role of Tissue and Systemic Hypoxia in Obesity and Type 2 Diabetes,” *J. Diabetes Res.* **2016**, 1527852 (2016).
 73. H. Thangarajah et al., “The molecular basis for impaired hypoxia-induced VEGF expression in diabetic tissues.,” *Proc. Natl. Acad. Sci. U.S.A.* **106**(32), 13505–13510 (2009).
 74. J. Ditzel and E. Standl, “The problem of tissue oxygenation in diabetes mellitus.,” *Acta Med. Scand. Suppl.* **578**, 59–68 (1975).
 75. R. Bucala, K. J. Tracey, and A. Cerami, “Advanced glycosylation products quench nitric oxide and mediate defective endothelium-dependent vasodilatation in experimental diabetes,” *J Clin Invest* **87**(2), 432–438 (1991).
 76. A. W. Stitt et al., “Elevated AGE-modified ApoB in sera of euglycemic, normolipidemic patients with atherosclerosis: relationship to tissue AGEs,” *Mol Med* **3**(9), 617–627 (1997).
 77. U. Chakravarthy et al., “Constitutive nitric oxide synthase expression in retinal vascular

- endothelial cells is suppressed by high glucose and advanced glycation end products,” *Diabetes* **47**(6), 945–952 (1998).
78. D. P. Stephens et al., “The influence of topical capsaicin on the local thermal control of skin blood flow in humans,” *Am J Physiol Regul Integr Comp Physiol* **281**(3), R894-901 (2001).
79. C. T. Minson, L. T. Berry, and M. J. Joyner, “Nitric oxide and neurally mediated regulation of skin blood flow during local heating,” *J Appl Physiol* **91**(4), 1619–1626 (2001).
80. D. L. Kellogg Jr., J. L. Zhao, and Y. Wu, “Roles of nitric oxide synthase isoforms in cutaneous vasodilation induced by local warming of the skin and whole body heat stress in humans,” *J Appl Physiol* **107**(5), 1438–1444 (2009).

Caption List

Fig. 1 The general scheme of the measuring system (A); localisation of the fibre optic probe with Peltier thermal-pad (B).

Fig. 2 Result of the modelling of diagnostic volume for the fluorescence measurements for the excitation wavelength of 365 nm (A) and 450 nm (B) for the parameters of the used optical fibre probe: the distance between the fibres – 1 mm, fibre diameter – 400 microns, receiving aperture angle – 0.22.

Fig. 3 The result of modelling the diagnostic volume for the LDF measurements for the wavelength of 1064 nm, using the following optical fibre probe parameters: distance between the fibres – 1.5 mm, receiving aperture angle – 0.22.

Fig. 4 Comparison of parameters between control (empty red bars), diabetic (loose blue shading) and diabetic with ulcers (tight green shading) groups: the normalised fluorescence amplitude (A) and the average perfusion in the stages of heating to 35 and 42 °C (B). In each box, the central line is the median of the group, while the edges are the 25th and 75th percentiles.

Fig. 5 The scatter plot with applied discriminant lines, obtained by linear discriminant analysis method (A) and ROC-curves for assessing the effectiveness of the classifiers (B). The healthy group is shown by squares, diabetic group – circles, the diabetic group with ulcers – triangles. For the ROC curve: red line – Control group vs Diabetic group 1, the blue line – Diabetic group 1 vs Diabetic group 2.

Table 1 Statistical difference between patient groups and data for controls.

Table 2 The results of experimental studies.

Table 3 Sensitivity and specificity for the first classification rule.